Wheel Force Transducer for Shimmy Investigation

D. De Falco, G. Di Massa *Member IAENG*, S. Pagano, S. Strano

***Abstract* — The paper presents two measuring systems to detect wheel lateral force that a castored tired-wheel exchanges with the ground during a shimmy oscillation. The force can be indirectly detected through the measure of the force that the wheel exchanges with the fork. Two measuring system have been proposed and tested; both systems introduce low mass transducers that do not influence the castor inertia characteristics. The first method is based on washer type load cells placed between fork and wheel while, the second one allows to estimate the tire lateral force by means of strain gauges placed on the fork sliders to detect the shear force.**

The paper describes the criteria followed to instrument a castored system constituted by a scooter front frame and the first experimental results for both systems.

***Index Terms*— Castor, Load cells, Shimmy, Strain gauge, Tire lateral force.**

I. Introduction

Measurement of the lateral force that a tired-wheel exchanges with the ground can be detected using wheel force transducers placed between wheel flange and wheel hub; these transducers, commercially available for vehicles [1], allow to measure the six components of the tire-ground interaction force but are generally bulky and heavy so that they involve a significant change of the system dynamic characteristics and cannot be used to measure the tire lateral force exerted by a low mass castor.

In order to estimate the lateral force that a lightweight castor exchanges with the road it is desirable to have a compact (not bulky) measurement system, adaptable to the castor geometry and lightweight, so that it can be mounted without substantial modifications of its components. Moreover, the lateral force measurement system does not induce a significant change of the inertial characteristics whose values are determinant for the system stability.

For a better understanding of the shimmy phenomenon [2] is useful to know the intensity of the lateral force and its phase delay with respect to the rotation angle of the castor. In fact, the lateral force can counteract or amplify the oscillation of the castor about its steering axis, in dependence of the phase delay with respect to the rotation.

D. De Falco is with the Second University of Naples, Italy (e-mail: domenico.defalco@unina2.it).

G. Di Massa is with the University of Naples Federico II, Italy (e-mail: gdimassa@unina.it).

S. Pagano is with the University of Naples Federico II, Italy (e-mail: pagano@unina.it).

S. Strano is with the University of Naples Federico II, Italy (e-mail: salvatore.strano@unina.it)

In the last case, self-excited oscillations of the system arises [3, 4].

The lateral force has a characteristic non-linear trend mainly depending on slip angle [5, 6]; in order to predict the operating conditions for which a castor is animated by self-excited oscillations and to preview its characteristics, in terms of amplitude and frequency, the lateral force must be suitably modelled [7].

Papers concerning experimental investigations on the shimmy phenomenon [8, 9] report the detections of the castor rotation around the steering axis or its angular acceleration. As it would be desirable to measure the tire lateral force intensity [10, 11], this paper describes an experimental investigation having the aim to estimate it. To this end, two measuring systems were tested on a test rig already adopted for experimental studies on the shimmy phenomenon [12].

The rig is constituted by a castor derived from a scooter front assembly, joined to a rigid steel frame by means of a support that allows the castor to vertically translate and to rotate around its steering axis. The support allows to adjust the rake angle and to apply a vertical load on the castor. The wheel rolls on a composite material belt, wrapped on two rolls, one of which is driven by an electric motor [13].

The castor suspension springs were removed and the sliders were connected to the tubes to avoid relative motion between sliders and tubes. In this way, the suspension elongation does not change with the vertical load and therefore the fork lateral stiffness can be considered constant in the different loading conditions.

The main castor characteristics are listed in Table I.

Fig. 1. Shimmy test rig.

ISBN: 978-988-14047-0-1
ISSN: 2078-0958 (Print); ISSN: 2078-0966 (Online)

TABLE I
CASTOR GEOMETRIC AND INERTIAL CHARACTERISTICS

Castor mass, m_c	30 kg
Wheel mass, m_w	8.3 kg
Wheel mass diametral moment of inertia, I_d	0.19 kgm^2
Wheel mass polar moment of inertia, I	0.32 kgm^2
Rake, ε	27°
Offset, d	48 mm
Trail, t	90 mm
Wheel radius, r	300 mm

The paper is organized as follows: sections II and III describe the lateral force estimation based on load cells and based on strain gouges, respectively; section IV illustrates static and dynamic tests with locked steer and section V describes the main results concerning tests with free steer.

II. LATERAL FORCE ESTIMATION BASED ON LOAD CELLS

The first measuring system is based on the following instrumentation (Fig. 2): a) two washer type load cells, arranged between fork sliders and wheel hub; b) two accelerometers, placed at the extremities of the wheel spindle; c) an angular transducer to measure the castor rotation around its steering axis.
Two rolling bearings, mounted on a tube coaxial to the wheel spindle, supports the wheel. Between tube and spindle there are two PTFE bushes allowing the wheel to translate along the spindle axis direction with low friction; the tube translation is constrained by the two washer-type load cells, arranged between the tube itself and the fork sliders (Fig. 3). The cells can only detect compressive loads and therefore the entire system was preloaded tightening the spindle; in such a way, a force acting on the wheel, parallel to the spindle axis, involves an increase of the compression in a load cell and the decompression of the other one. The difference of two load cells signals gives the force acting on the wheel.

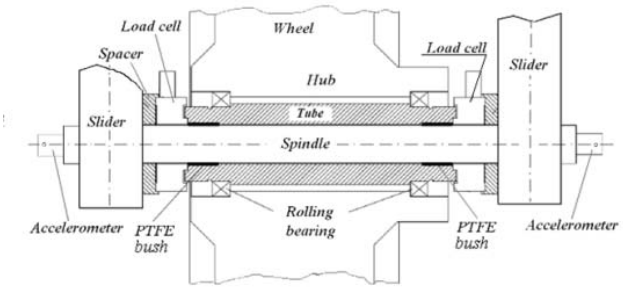

Fig. 2. Scheme of the wheel force transducer.

Fig. 3. Load cell and accelerometer.

The cells are loaded by the tire lateral force and even by the lateral wheel inertia force; to distinguish the two contributions, the latter was estimated assuming that the wheel lateral acceleration is equal to the axial spindle acceleration, measured by means of two accelerometers placed at its extremities (Fig. 3).

Adding the two accelerometer signals, the following acceleration is detected (Fig. 4):

$$a_2 = (a_{tL} + a_{tR} - a_{cL} + a_{cR})\cos\beta + a_{yL} + a_{yR} = a_{tL}\cos\beta + a_{tR}\cos\beta + a_{yL} + a_{yR} \quad (1)$$

where the subscript t and c stand for *tangential* and *centripetal* while L and R stand for *left* and *right*. The acceleration expression highlights that, adopting two accelerometers, the centripetal acceleration component vanishes.

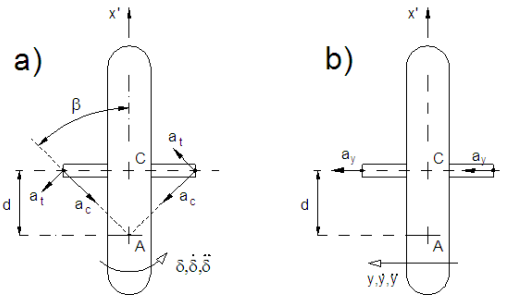

Fig. 4. Acceleration components.

Furthermore, since:

$$a_{tL} = a_{tR} = a_t \qquad a_{cL} = a_{cR} = a_c \qquad a_{yL} = a_{yR} = a_y \quad (2)$$

it follows:

$$a_2 = 2a_t\cos\beta + 2a_y\,. \quad (3)$$

where a_t component can be deduced from the castor angular sensor.
Expression (3) highlights that, adding the two accelerometer signals, it is detected twice the lateral acceleration due to the lateral wheel motion and to the component of the tangential acceleration that arises during the castor rotation. The lateral acceleration results:

$$a = a_2/2 = a_t\cos\beta + a_y \quad (4)$$

An amount of the tire lateral force is contrasted by the the friction forces acting in the PTFE busches (Fig. 2) and therefore is not measured by the load cells. This amount depends on the radial forces acting on the bushes that, in turn, depends on: *a*) wheel weight; *b*) moment due to the lateral force that arises in the contact patch area; *c*) wheel inertia couple; *d*) gyroscopic couples due to the rotation of the castor around the steering axis and due to the lateral flexibility of the fork. The bushes are also subjected to: *e*) vertical forces of inertia due to the castor center of mass vertical motion caused by steering rotation; *f)* radial force due to the unbalance of the wheel.
An expertimental investigation was conducted to evaluate the method complexity; Fig. 5 reports the steering signal,

ISBN: 978-988-14047-0-1
ISSN: 2078-0958 (Print); ISSN: 2078-0966 (Online)

and the estimated tire lateral force obtained perturbing the castor in free steer condition. The test was performed in stable operation condition but near the stability threshold. Fig. 6 highlights the delay of the steering angle with respect to the lateral force; the two signals are reported in the same diagram in a normalized scale.

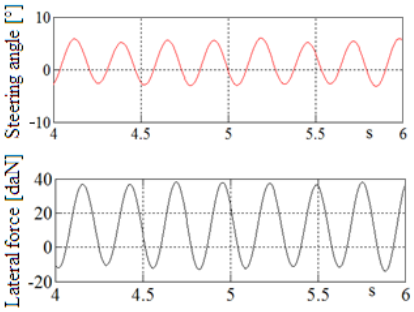

Fig. 5. Shimmy oscillation at 20 km/h.

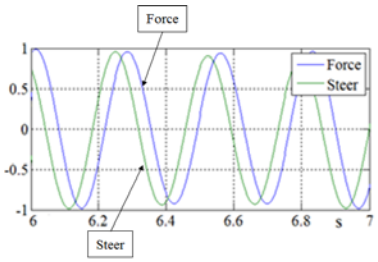

Fig. 6. Delay of the force with respect to the steering angle.

The acceleration detected at the extremities of the wheel spindle (Fig. 7) shows low values until the steer angle is zero; then the acceleration is characterized by a beat due to the closeness of the two castor natural bending frequencies. The two modes have frequencies equal to about 13.8 Hz and 15.5 Hz respectively as shown by the FFT reported in the same figure; the beat period is therefore equal to about: $T_b=1/(f_2-f_1)$=0.6s.

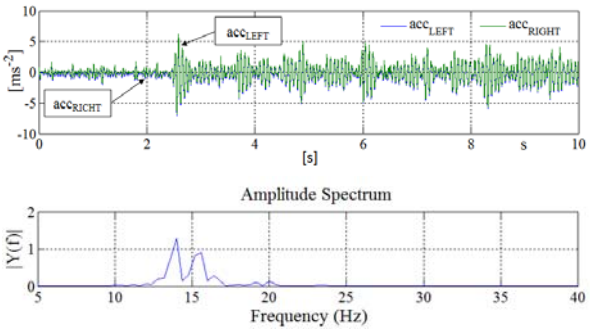

Fig. 7. Accelerometer signal and its FFT.

Tire lateral force depends on the vertical load acting on the wheel, given by the sum of the weight and by two periodic inertia forces, attributable to:

a) the wheel unbalance, acting with frequency corresponding to the wheel rotation speed;
b) the center of gravity height variation, due to the castor rotation around the steering axis; this acceleration has a frequency f_b, twice the frequency of shimmy.

For the reported test, considering a forward velocity V = 20 km/h (5.55 m/s) and a wheel radius R equal to about 0.28 m, the frequency synchronous with the wheel rotation results: $f_a = V/(2\pi R) = 3.2$ Hz . The shimmy oscillation, at 4.5 Hz, causes a periodic vertical load, with a frequency equal to about f_b = 9 Hz.

Even the horizontal acceleration is constituted by two periodic component, both due to the castor rotation around the steer axis. The first component is synchronous with the shimmy oscillation while the other one is the centripetal acceleration that has a frequency that is twice the shimmy frequency; in fact, assuming a castor harmonic rotation, $\theta(t) = \Theta \cdot \sin(\omega t)$, with circular frequency ω, the expression of the centripetal acceleration is characterized by a 2ω circular frequency:

$$a_c(t) = e \cdot \dot{\theta}^2(t) = e \cdot \omega^2 \Theta^2 \frac{\cos(2\omega t)+1}{2} = \\ = \frac{e\omega^2\Theta^2}{2}\left(1+\frac{e\omega^2\Theta^2}{2}\cos(2\omega t)\right) \quad (5)$$

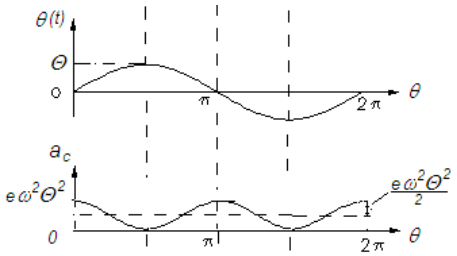

Fig. 8. Castor centripetal acceleration

At 20 km/h, the maximum acceleration value detected by the accelerometers, placed on the spindle extremities, is about 8 ms^{-2}.

The proposed method allows the estimation of the tire lateral force but requires many sensors and several signal processing operations; in any case, the estimated values is affected by the uncertainty due to friction between spindle and PTFE bushes. For this reason, an alternative method is proposed in the next paragraph.

III. Lateral Force Estimation Based on Strain Gouges

Tire lateral force can be estimated by measuring the shear strain of the fork sliders by means of strain gages; lateral shear force acting on the fork is equal to the lateral force that tire exchanges with road. To this end, each fork slider was instrumented with two strain gages to detect the shear force (the front ones are visible in Fig. 9).

Fig. 9. Fork sliders instrumented with strain gauge.

ISBN: 978-988-14047-0-1
ISSN: 2078-0958 (Print); ISSN: 2078-0966 (Online)

Each slider-tube system was calibrated by horizontally fixing the tube and applying a vertical static load at the extremity of the slider (Fig. 10).

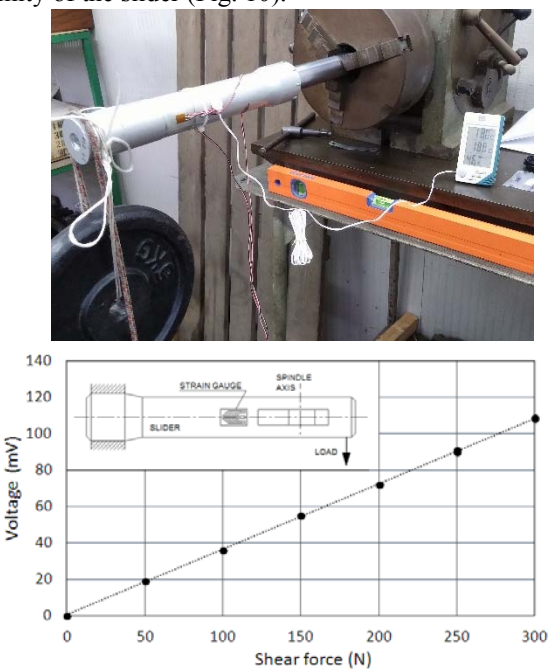

Fig. 10. Slider calibration curve.

Dual-grid biaxial strain gauge were employed; each one has two sensible elements positioned to detect strain along to ± 45 ° to the direction of shear force.

As said in the introduction, the fork tubes were locked to the sliders by means of mechanical locking bushes so that the fork geometry and therefore the fork lateral stiffness do not change with the vertical load.

IV. Static and Dynamic Tests with Locked Steer

A first serie of tests was conducted with the wheel raised from the flat track belt and castor rotation restrained (locked steer). In this condition the system was horizzontaly loaded by a shaker in correspondence of the wheel axis (Fig. 11).

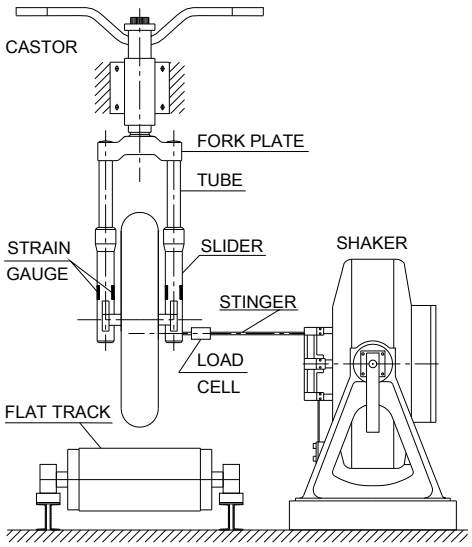

Fig. 11. Castor excited by the shaker.

In this configuration, the castor was preliminarly subjected to a sequence of increasing static lateral loads feeding the shaker with direct current; for each load step, the shear forces detected by the two sliders were plotted versus the fload exerted by the shaker. Fig. 12 shows that the calibration curve of the measuring system is almost linear and that the two sliders exhibit the same response (the two curves are overlapped in Fig. 12).

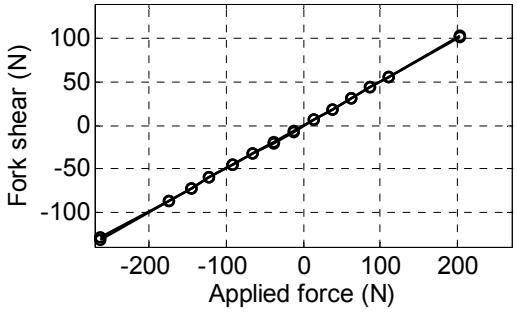

Fig. 12. Calibration of the mounted fork.

The fork dynamic response was highlighted by applying a sequence of steady state horizontal harmonic forces with different frequencies; Fig. 13 reports the ratio between the amplitudes of the shear force, measured by the strain gauges, and the force amplitude exerted by the shaker.
Up to the lateral bending resonance frequency, occurring at about 14.5 Hz, the system has an almost linear behavior, characterized by a low damping level. The signals coming from the two sliders are in phase and have the same amplitude up to the frequency of 22 Hz.

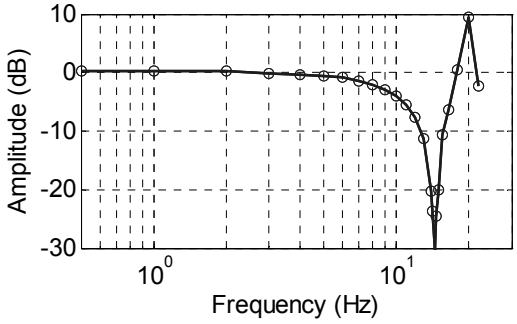

Fig. 13. Fork harmonic response with no contact between tire and belt.

The same test was repeated with the wheel leaning on the flat track belt at rest and loaded by its own weight and with an adding vertical load equal to 400N. In this case (Fig. 14) for the presence of the tire reaction the resonance frequency is shifted at slightly higher values (19.0 Hz in case of no adding load and 20.5 Hz with an adding load of 400 N) and, even in this case, the two signals are almost overlapped up to a frequency of about 22 Hz .

ISBN: 978-988-14047-0-1
ISSN: 2078-0958 (Print); ISSN: 2078-0966 (Online)

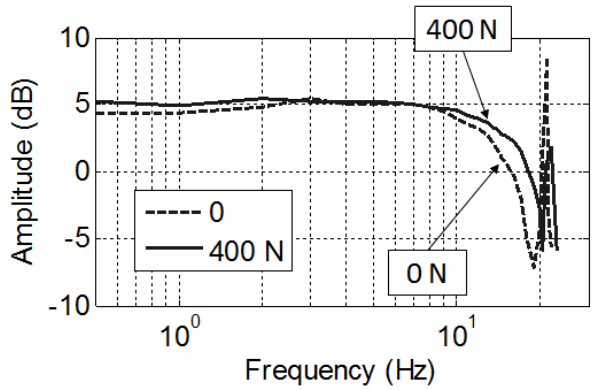

Fig. 14. Fork harmonic response with flat track at rest.

Finally, the test was repeated with the flat track translating at 10 km/h, with an adding load of 400N. The obtained curve (Fig. 15) is compared with the previous ones to highlight that the dynamic response is similar to the first test (no contact between belt and wheel) for low exciting frequency while the response slightly approaches to that of the second test (wheel leaning on the flat track at rest) for increasing frequencies. When the wheel rolls, lateral tire reaction depends on slip angle which in turn depends on the lateral velocity and therefore on the frequency of the lateral motion.

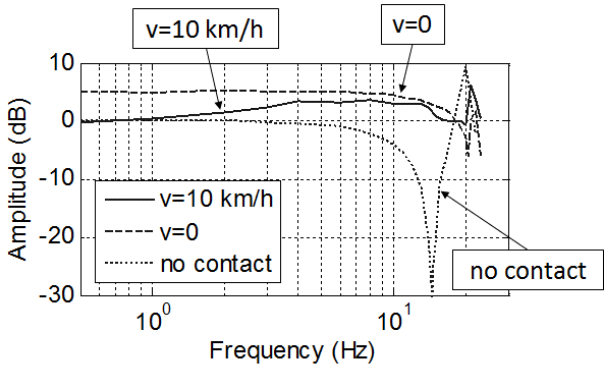

Fig. 15. Fork harmonic response with flat track moving at 10 km/h.

The fork was shortned by reducing the fork tube extension (Fig. 11) from 220 mm to 180 mm, to obtain a stiffer and a more stable castor with respect to the shimmy phenomenon. In raised wheel configuration the fork was excited with a sweep-sine force (frequency variation: 1 Hz/s) to evaluate the relative resonant frequency; the correspondent FRF (Fig. 16) shows that the first natural frequency occurs at 15.2 Hz.

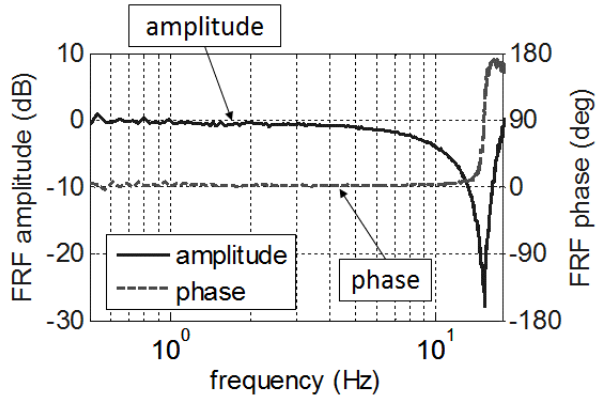

Fig. 16. Sweep response.

Furthermore, the signals coming from each slider have the same phase up to a frequency of about 23 Hz (see Fig. 17) and therefore they may be summed to provide the total shear force. The measuring system can be properly adopted to study the shimmy phenomenon as the castor adopted for the tests derives from a motorcycle fork and therefore the shimmy phenomenon occurs at a frequency that is lower than 10 Hz (as experimentally shown in Figg. 19 - 21).

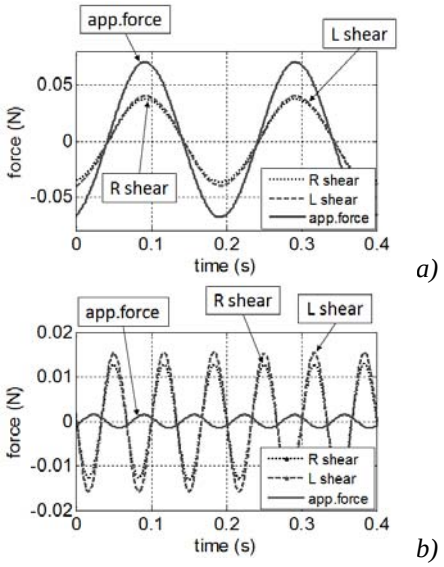

Fig. 17. Applied force and fork shear: a) 5 Hz; b) 10 Hz.

V. Free Steer Tests

Some tests were performed by assigning to the belt of flat track (Fig. 18) a constant speed and an adding vertical load of 200 N. The castor was left free to rotate around the steering axis and was perturbed by means of an impulsive force applied to the handlebar, at different belt velocity, to check if a damped or an undamped oscillation arises.

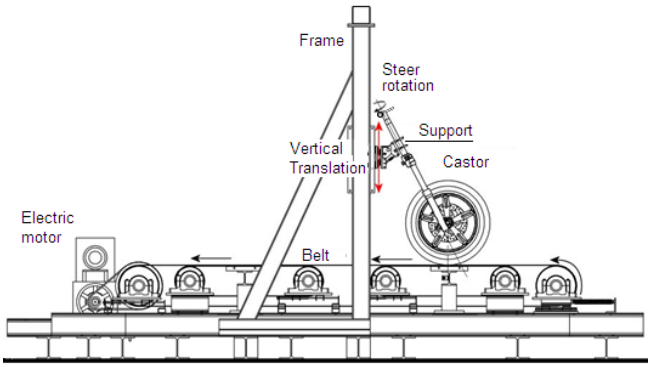

Fig. 18. Castor on flat track.

In [3] it is shown that shimmy phenomenon can be interpreted by means of 3 d.o.f mathematical model. The characteristics of the relative vibrating modes (frequency and damping) depend on the castor forward speed; the model exhibits that, in several range velocity, one or more modes may be characterized by a negative damping (unstable). In particular, castors having low lateral stiffness are characterized by a mode that is unstable at low forward speed. For higher speeds, this mode recovers stability but, if the forward speed exceeds a threshold value, another mode

ISBN: 978-988-14047-0-1
ISSN: 2078-0958 (Print); ISSN: 2078-0966 (Online)

becomes unstable and, for further velocity increments, the system does not recover spontaneously stability. Stability may be recovered in several ways as, for example, modifying the castor stiffness, the tire sideslip stiffness coefficient, the steering damping, the inertia castor, etc.
The results of the tests are reported in terms of steer rotation and tire lateral force. In particular, Fig. 19 reports an unstable operating condition occurring at 10 km/h. The castor oscillates with a frequency of about 3.6 Hz and its angular position is almost in phase with the tire lateral force.

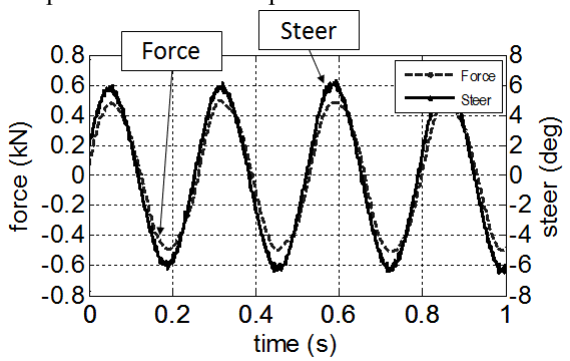

Fig. 19. Castor on flat track running at 10 km/h.

At a forwad speed of 57 km/h, the castor does not oscillate until it is perturbed; then a self-excited oscillation arises at a frequency of about 5.6 Hz (Fig. 20).

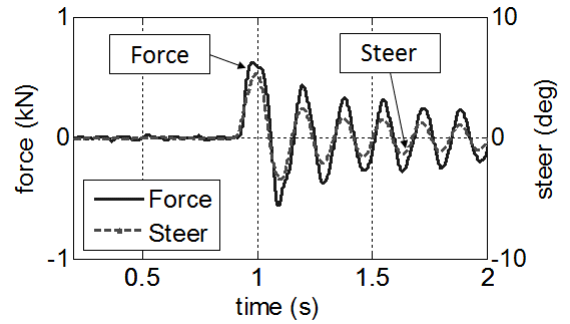

Fig. 20. Castor on flat track running at 57 km/h.

The last test was performed at 60 km/h; the castor behaviour is stable and the pertubation induces a damped oscillation (Fig. 21).

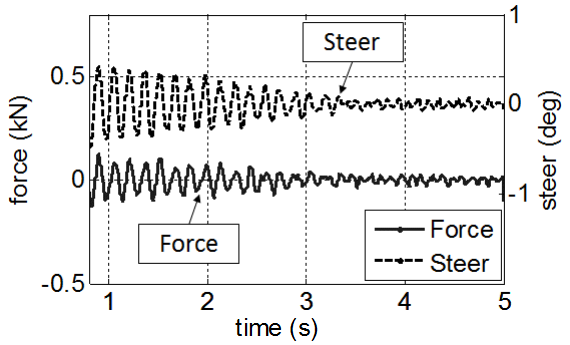

Fig. 21. Castor on flat track running at 60 km/h.

VI. Conclusions

The paper presents two measuring systems to estimate the lateral force that the tire of a castor exchanges with the road.
The first system, mainly based on the use of load cells disposed between fork and wheel, requires more measuring instruments and a more demanding signal processing; it is also affected by the uncertainty related to the friction forces even if of small entity.
The second system, based on the use of strain gauges on the sliders, can be suitably adopted for the study of the shimmy phenomenon.

Acknowledgments

The authors are grateful to ing. M. Di Pilla, G. Iovino, G. Stingo and ing. M. Pontecorvo for their collaboration during the execution of laboratory tests.

References

[1] http://www.pcb.com/Linked_Documents/AutomotiveSensors/LT_WFT_Lowres.pdf
[2] H.B. Pacejka, Analysis of the shimmy phenomenon, Proceedings of the Institute of Mechanical Engineers: Automobile Division , Vol. 180, n. 1, pp.251-268, January 1965
[3] D. De Falco, G. Di Massa, S. Pagano, "On castor dynamic behavior", Journal of the Franklin Institute n.347, 2010, pp. 116–129;
[4] G. Di Massa, S. Pagano, S. Strano, M. Terzo - A stability analysis of the wheel shimmy – in Proc. of the ASME 11th Biennial Conference on Engineering Systems Design and Analysis, (ESDA), Vol. 1, pp. 669 – 678, Nantes, France, july 2-4, 2012.
[5] Lynn C. Rogers. "Theoretical Tire Equations for Shimmy and Other Dynamic Studies", Journal of Aircraft, Vol. 9, No. 8, pp. 585-589, 1972
[6] H.B. Pacejka, E.Bakker: The Magic Formula Tire Model, Vehicle System Dynamics, Vol.21 supplement, 1993.
[7] D. de Falco, S. della Valle, G. Di Massa, S. Pagano, The influence of the tyre profile on motorcycle behaviour, Supplement of *Vehicle Systems Dynamics*; vol.43, 2005, pp. 179-183.
[8] D. Takács, G. Stépán, Experiments on Quasiperiodic Wheel Shimmy, *Journal of Computational and Nonlinear Dynamics*, vol. 4/031007-1, 2009
[9] D. de Falco, G. Di Massa, S. Pagano - Wheel shimmy experimental investigation – ASME 2012, 11th Biennal Conference on Engineering systems Design and Analysis (ESDA) Vol.1, pp. 717-726 –, july 2-4, 2012
[10] L. Feng, G. Lin, W. Zhang, H. Pang, T. Wang, Design and optimization of a self-decoupled six-axis wheel force transducer for a heavy truck, *Proceedings of the Institution of Mechanical Engineers*, Part D: Journal of Automobile Engineering, 2015.
[11] G. Di Massa, S. Pagano, S. Strano, M. Terzo - A mono-axial wheel force transducer for the study of the shimmy phenomenon - World Congress on Engineering (WCE), (ISBN: 978-988-19251-0-7) - London, U.K., 3-5 July, 2013.
[12] D. De Falco, G. Di Massa, S, Pagano - Castor Dynamic Investigation - International Review of Mechanical Engineering, Vol. 7, N. 3, pp. 527-533, March 2013.
[13] D. De Falco, G. Di Massa, S, Pagano - A Full Scale Motorcycle Dynamic Rig - International Review of Mechanical Engineering, Vol. 7, N. 3, pp. 519-526, March 2013.